Tribol. Lubr., Vol. 34, No. 6, December 2018, pp. 300~306
Tribology and Lubricants

ISSN 1229-4845(Print) • 2287-4666(Online)
http://Journal.tribology.kr

DOI https://doi.org/10.9725/kts.2018.34.6.300

Testing of Load Capacity of a Foil Thrust Bearing

Choong Hyun Kim† and Jisu Park

Center for Bionics, Bionics Research Institute, Korea Institute of Science and Technology

(Received October 3, 2018; Revised November 24, 2018; Accepted November 28, 2018)

Abstract – In this study, the performance of foil thrust bearings was investigated by performing bearing take-off and load capacity tests, using an in-house designed and manufactured vertical bearing test rig. The mean take-off rotational speed and maximum load capacity of the bearing specimen were ~18,000 rpm and ~80 kPa, respectively. The vertical bearing test rig was observed to yield higher coefficients of friction and frictional torques than a horizontal bearing test rig under identical test conditions. This was a result of its structural characteristics, in that the bearing specimen is placed atop the thrust runner, which keeps it from being separated from the runner after the bearing take-off. In addition, bearing take-off was observed at a higher runner rotational speed as this structure keeps air from flowing between the top foil and runner surfaces, which requires a higher runner speed. The parallel alignment between the bearing specimen and runner surfaces can be maintained within a certain range more easily in a vertical test rig than in a horizontal test rig. Because of these advantages, Korean Industrial Standard, KS B 2060, recommends a vertical bearing test rig as the standard test device for foil thrust bearings.

Keywords – foil thrust bearing, vertical bearing test rig, take-off, bearing torque, load capacity

1. Introduction

Foil bearings are air-lubricated bearings widely used for high-speed turbomachinery because of their advantages of a simple structure coupled with low friction operation. They are categorized into two types depending on the direction of the primary load: foil journal bearings designed to support radial loads, and foil thrust bearings designed to support axial loads.

The US Army Research Laboratory [1] conducted performance testing of high-speed foil thrust bearings designed to operate at high speed under high-temperature conditions. Dykas [2] and Stahl [3] reported performance of foil thrust bearings under varying operating conditions. Kim et al. [4] reported foil thrust bearings using an in-house-developed horizontal test rig.

The Korea Institute of Science and Technology developed a foil thrust bearing performance testing method and published it as Korean Industrial Standard, KS B 2060 [5].

In this study, performance testing of foil thrust bearings (hereafter "bearings") was conducted using an in-house-developed vertical test rig, with bearing torque, load capacity, and bump foil surface temperature (hereinafter "bearing surface temperature") as performance parameters.

2. Test Setup and Bearing Specimen

2-1. Test rig configuration

Fig. 1 shows a schematic of the test rig used in this study. It comprises four vertically arranged components: runner (7), load transfer unit (3, 4), load cell (2), and loading plate (1). The runner is driven by an electric motor (8) with a rated power of 30 kW and a maximum speed of 30,000 rpm.

†Corresponding author: nems.kim@gmail.com
Tel: +82-2-958-5668, Fax: +82-2-958-5629
http://orcid.org/0000-0002-0162-6342

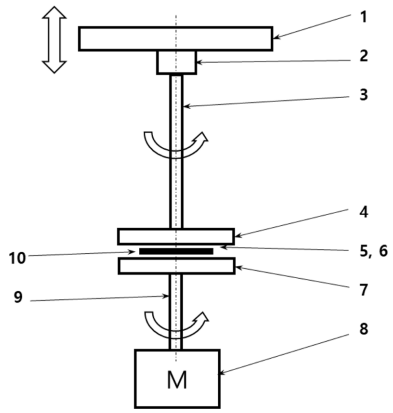

Fig. 1. Test rig for performance testing of foil thrust bearing: 1 - loading plate, 2 - load cell, 3 - loading shaft, 4 - mounting disk for bearing specimen, 5 - thermocouple for measuring air temperature, 6 - thermocouple for measuring bump foil surface temperature, 7 - runner, 8 - electric motor, 9 - driving shaft, 10 - bearing specimen.

Rubber anti-vibration pads and air pads were stacked between the test rig and the floor to minimize vibration transmission from the floor.

2-1-1. Loading unit

The bearing test rig, as shown in Fig. 1, provides vertical motion of the loading plate along the axis of rotation. The axial load applied to the bearing specimen can be constrained by controlling the clearance between the bearing specimen (10) and the runner when the loading plate descends towards the runner.

The unit transferring the load applied to the bearing specimen to the load cell is installed above the bearing specimen. It comprises a loading shaft and a mounting disk for the bearing specimen, whose total weight of 13.4 N is defined here as the "basic axial load," given that it is a constant load acting on the bearing specimen. The alignment between the specimen and the runner can be adjusted by limiting the position of the loading shaft using air bushing around the loading shaft.

2-1-2. Test method

In Fig. 1, a bearing specimen, which is fixed to the mounting disk and connected to the loading shaft, is moved downward so that it contacts the surface of the runner. An initial load, which is measured by the load cell, is applied by thrusting the loading plate toward the runner. The electric motor then rotates the runner, generating friction between the specimen and the runner. When the runner reaches a certain speed, an air film is formed between the bearing specimen and the runner, which causes the bearing to take off and separate from the runner. The following bearing performance parameters were measured during each take-off test cycle: rotational speed of the runner, axial load applied to the specimen, torque generated by friction between the runner and the top foil, and the temperature of the bump foil surface. The testing was conducted at room temperature.

2-1-3. Data collection

The axial load applied to the bearing specimen during testing was measured using a 6-axis load cell installed beneath the loading plate. The total axial load acting on the specimen (hereinafter "net load") was calculated by adding the abovementioned basic axial load to the value measured by the load cell. Because the 6-axis load cell is connected to the loading shaft, the rotational torque generated by the bearing rotation can also be measured.

The rotational speed of the runner was measured using the control signal of the motor driver. In addition, a separate optical tachometer was installed to directly measure the rotational speed of the driving shaft. The measured values were then compared to check the measurement accuracy. The load and torque data collected were processed through a low pass filter (20 Hz) for analysis.

2-2. Bearing specimen

Fig. 2 shows the configuration of the bearing specimen. The bearing comprises a bearing plate (12), a bump foil (13) fixed to the bearing plate to provide the bearing stiffness, and a top foil (14) placed over the bump foil and facing the runner to

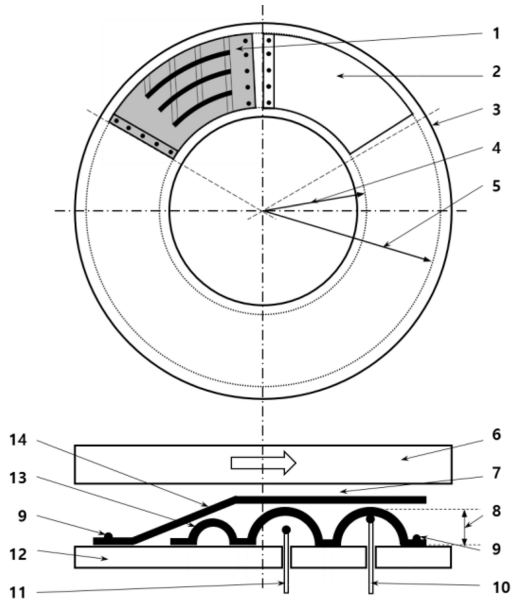

Fig. 2. Schematic of foil thrust bearing: 1 - bump foil, 2 - top foil, 3 - bearing plate, 4 - inner radius of top foil, 5 - outer radius of top foil, 6 - runner, 7 - air film, 8 - bump height, 9 - welding point, 10 - thermocouple for measuring bump foil surface temperature, 11- thermocouple for measuring air temperature, 12 - bearing plate, 13 - bump foil, 14 - top foil.

Table 1. Specification of bearing specimen

Parameter	Value
Number of top foils	6
Bump height (mm)	0.5
Young's modulus of foil (GPa)	210
Poisson's ratio	0.3
Area of top foil, total (mm^2)	3,500

form an air film and directly exposed to the axial load.

The surface of the top foil of the bearing specimen was coated with polytetrafluoroethylene, a self-lubricating material with excellent heat resistance and a low friction coefficient.

3. Performance Testing

3-1. Take-off testing

Changes in the bearing torque were observed during take-off testing while rotating the runner. Each take-off test cycle of 20 s comprised four phases: 4 s to accelerate the runner from standstill to 25,000 rpm, 6 s maintaining the maximum speed, 4 s to decelerate the runner from 25,000 rpm to standstill, and 6 s at the touchdown state.

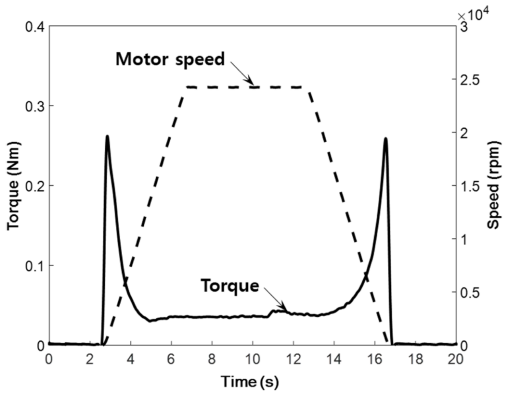

Fig. 3. Take-off test with runner speed up to 25,000 rpm.

The measured torque had three components: start-up torque (the maximum torque when the runner starts to rotate), bearing torque (the torque at the moment of separation of the runner and top foil when the bearing lifts off, with the thickness of the air film maintained constant by the runner rotating at a high speed), and touch-down torque (the maximum torque when the rotating runner stops rotating and the specimen lands back on the runner surface).

In the take-off testing, the runner was rotated with an initial load of 2.5 N acting on the load cell atop the specimen. Considering the basic axial load of 13.4 N, the net load acting on the bearing specimen was 15.9 N, and the pressure applied to the top foil surface was 4.3 kPa.

A total of 2,000 take-off test cycles were applied to the bearing specimen, and the bearing torque was averaged every 500 cycles and changes were noted. Fig. 3 shows the average torque measured from 1,501 to 2,000 take-off test cycles.

As can be seen in Fig. 3, the start-up torque is

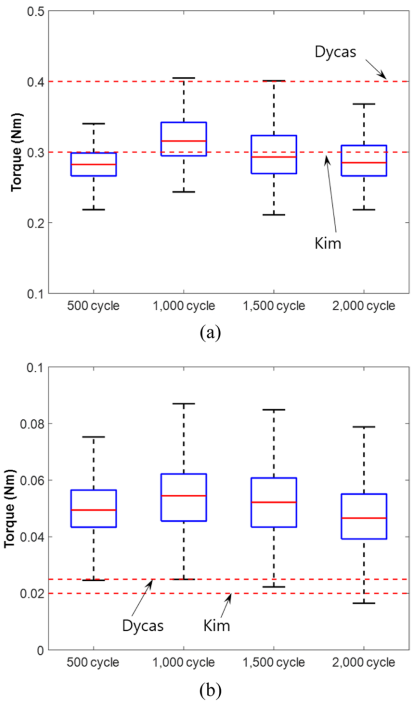

Fig. 4. Comparison of torque variations between foil thrust bearings: (a) start-up torque (b) bearing torque.

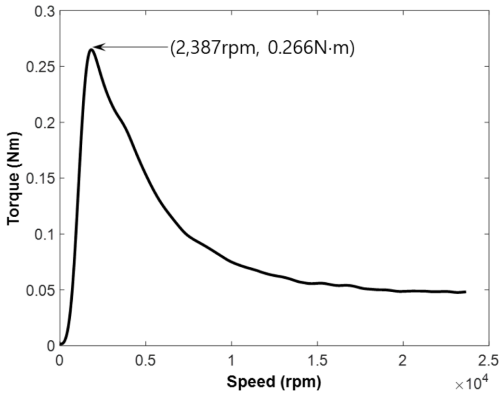

Fig. 5. Variation of torque vs runner speed up to 25,000 rpm: averaged torque values of start-stop test from 501 to 2,000 cycles.

in the range 0.28~0.3 N·m. When the runner accelerates to a stable operating range, the bearing torque decreases to ~0.05 N·m. This is attributable to reduced friction because of an air film formed between the runner and the bearing top foil surface by the hydrodynamic pressure generated by the high-speed rotation of the runner as a result of bearing take-off. When the runner stops rotating, the torque value increases abruptly toward the touch-down torque value. The touch-down and start-up torques were similar.

We compared the measured start-up and bearing torques with those reported by Dykas [2] and Kim et al. [4] in Fig. 4.

As can be seen in Fig. 4(a), the mean start-up torque in this study is smaller than that of Dykas [2] (0.4 N·m) and similar to that of Kim et al. [4] (0.3 N·m).

The start-up torque, with a mean value of 0.28 N·m in the first 500 take-off test cycles, increased marginally to 0.31 N·m between 501 to 1,000 cycles, and decreased back to 0.27 N·m after 2,000 cycles. From this it can be inferred that, after repeated increases and decreases during running-in between the top foil and runner surfaces in the initial test stage, the torque value stabilized after 2,000 cycles.

Fig. 4(b) shows the mean bearing torque generated in the stable operating range every 500 cycles after bearing take-off. The mean bearing toque obtained was more than double those reported by Dykas [2] and Kim et al. [4] (0.05 N·m vs. 0.025 N·m and 0.02 N·m, respectively). This is indicative of the generation of greater frictional forces between the bearing specimen and runner even after the formation of an air film between them.

These differences in frictional torque are surmised to be a result of the structural differences between the test rigs used, given that Dykas [2] and Kim et al. [4] used horizontal test rigs as opposed to the vertical test rig used in this study. It is surmised that the even and close contact between the top foil and runner surfaces facilitated the contact between them being maintained, even after bearing take-off in the vertical bearing test rig, and resulted in the greater frictional torques compared to the horizontal test rig under identical test conditions.

Fig. 5 shows the mean torque generated in the initial phase of the bearing take-off testing from 1,501 to 2,000 cycles. It can be seen that the start-up torque of 0.27 N·m was rapidly attained at approximately 2,400 rpm, and gradually decreased to 0.05 N·m when the runner rotational speed exceeded 18,000 rpm. Given that this minimum torque value appears after the formation of an air film between the bearing top foil and runner surfaces, 18,000 rpm can be considered to be the bearing take-off speed.

In a comparable study by Kim et al. [4] using bearing specimens with similar specifications, the bearing take-off speed was 13,000 rpm, approximately 28% lower than in this study. As discussed above, the reason for this difference in bearing take-off speed is considered to be the structural differences between the vertical and horizontal bearing test rigs. The former allows a closer contact between the specimen and runner, therefore, preventing the inflow of sufficient air required for the formation of an air film between their surfaces. In this case, a greater hydrodynamic pressure, i.e., higher runner speed, is required for the bearing to take off.

3-2. Load capacity testing

Load capacity testing was conducted by lowering the loading plate toward the specimen, thereby increasing the load acting on the bearing. This was preceded by the bearing take-off by accelerating the runner from standstill to 25,000 rpm with a preload applied to the bearing specimen.

The load measured at the moment of the initial failure of the coating layer because of friction was defined as the maximum load capacity. The time of the coating failure was determined using the odor produced by coating layer oxidation, as well as changes in the bearing torque and bearing surface temperature.

Fig. 6 shows the time-dependent variations in (a) axial load (pressure), (b) torque, and (c) bearing surface temperature from data collected during a load capacity test.

From the results of the three tests it was observed

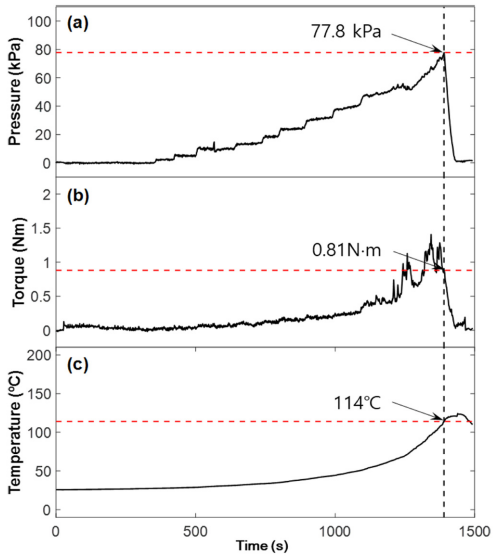

Fig. 6. Typical bearing test data during load capacity test under 25,000 rpm runner rotational speed: (a) load, (b) torque, and (c) temperature.

that the bearing specimen failed under a net load of ~80 kPa (79.4±2.0 kPa), with the bearing torque 1.0±0.3 N·m. The surface temperature of the bearing specimen increased to 107±11.5°C at the maximum load capacity, which was 85±11.5°C higher than the baseline temperature. When compared to the results of Kim et al. [4], the difference in the maximum load capacity was negligible, however, the bearing torque and bearing surface temperature were significantly greater. As mentioned above, the high frictional force generated between the top foil and the runner surfaces is assumed to induce a substantial increase not only in the bearing torque, but also in the bearing surface temperature under the same load.

Fig. 7 shows an abrupt increase in the bearing torque generated after bearing take-off at loads greater than 50 kPa. This is assumed to be because of an abrupt increase in the frictional force because of the closer contact between the top foil surface of the bearing specimen and the runner surface. In this case, part of the surface is outside the fluid lubrication region.

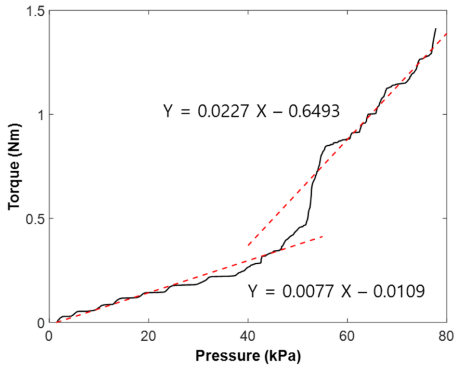

Fig. 7. Torque vs load during load capacity test under 25,000 rpm runner rotational speed.

Fig. 8. Bearing specimen after load capacity test.

The equations for the relationship between load and torque in the load ranges <50 kPa and ≥50 kPa exhibited linear relationships with different slopes: the slope of the graph increases by three times.

Fig. 8 shows the surface of a bearing specimen after the load capacity test. The Teflon coating layer on the top foil surface is partially peeled off. In the <50 kPa load range, the coating layer exhibited some traces of friction, but no coating failure. This suggests that load increases in the ≥50 kPa load range because of external disturbances will, in all probability, lead to bearing failure.

4. Conclusions

In this study, the performance of foil thrust bearings was investigated by conducting bearing take-off and load capacity tests, using an in-house-developed vertical bearing test rig.

The mean take-off speed and maximum load capacity of the bearing specimen were ~18,000 rpm and ~80 kPa, respectively. It was also observed that the test rig operated at a low-friction state with a mean coefficient of friction as low as 0.05 N·m or less after take-off.

Regarding the overall performance evaluation, the vertical bearing test rig was assumed to yield higher torques compared to a horizontal bearing test rig under identical test conditions because of its structural characteristics where the bearing specimen is placed atop the thrust runner, which allows the maintenance of close contact between the specimen and runner after bearing take-off. The friction torque can be reduced by appropriately adjusting the alignment between the test piece and the runner.

In addition, the bearing take-off occurs at a higher runner rotational speed, which could be a result of the structure keeping air from flowing between the top foil and runner surfaces, which necessitates a greater hydrodynamic pressure, i.e., higher runner speed, for bearing take-off.

Acknowledgements

This study was supported by a grant from the National Standard Technology Improvement Project of the Ministry of Commerce, Industry and Energy (Project No. 10058942).

References

[1] Army Research Laboratory, “A Foil Thrust Bearing Test Rig for Evaluation of High Temperature Performance and Durability,” ARL-MR-0692, April 2008.

[2] Dykas, B. D., “*Factors Influencing the Performance of Foil Gas Thrust Bearings for Oil-Free Turbomachinery Applications*,” Thesis for the degree of Doctor of Philosophy, Case Western Reserve University, May, 2006.

[3] Stahl, B. J., “*Thermal Stability and Performance of Foil Thrust Bearings*,” Thesis for the degree of Mas-

ter of Science, Case Western Reserve University, May 2012.
[4] Kim et al., "Experimental study on the load carrying performance and driving torque of gas foil thrust bearings," *J. Korean Soc. Tribol. Lubr. Eng.*, Vol. 31, No. 4, pp. 141-147, 2015.
[5] KS B 2060:2016, "Hydrodynamic Oilless Plain Bearing – Foil Thrust Bearing – Evaluation of Static Load Capacity, Friction Coefficient and Lifetime," December 2016.